Intramolecular Interactions in the N-Domain of Cardiac Troponin C Are Important Determinants of Calcium Sensitivity of Force Development†

Karen L. Reece and Richard L. Moss*

Department of Physiology, University of Wisconsin School of Medicine and Public Health, 123 Service Memorial Institute, 1300 University Avenue, Madison, Wisconsin 53706

Received January 29, 2008; Revised Manuscript Received March 10, 2008

ABSTRACT: Myocardial contraction is initiated when Ca^{2+} binds to site II of cardiac troponin C. This 12-residue EF-hand loop (NH_2-**D***E***D**G***S***G***T***V**D***FD***E**-COOH) contains six residues (bold) that coordinate Ca^{2+} binding and six residues that do not appear to influence Ca^{2+} binding directly. We have introduced six single-cysteine substitutions (italics) within site II of cTnC to investigate whether these residues are essential for Ca^{2+} binding affinity in isolation and Ca^{2+} sensitivity of force development in single muscle fibers. Ca^{2+} binding properties of mutant proteins were examined in solution and after substitution into rat skinned soleus fibers. Except for the serine mutation, cysteine substitution had no effect on Ca^{2+} binding on c*T*nC in solution. However, as part of the myofilament, the threonine mutation reduced Ca^{2+} sensitivity while the phenylalanine mutation increased Ca^{2+} sensitivity. Analysis of the available crystal and NMR structures reveals specific structural mechanisms for these effects.

Force development in myocardium is regulated by a number of interactive processes, including Ca^{2+} binding to regulatory proteins, the activating effects of crossbridge binding to actin, and the modulation of activation by phosphorylation of myofibrillar proteins (*1, 2*). Ca^{2+} binding to the regulatory protein cardiac troponin C (cTnC)[1] initially switches on the thin filament by causing a conformational change in the troponin−tropomyosin complex that allows crossbridges to bind to actin. cTnC is an EF-hand protein with two structural, high-affinity Ca^{2+}/Mg^{2+} binding sites (sites III and IV) at the C-terminus ($K_{Ca^{2+}} \approx 10^7$ M^{-1}; $K_{Mg^{2+}} \approx 10^3$ M^{-1}) (*3*) and two low-affinity Ca^{2+} binding sites at the N-terminus (sites I and II); however, site I is inactive due to key amino acid substitutions in the binding loop (*4*). The low-affinity site (site II) binds Ca^{2+} on the order of 10^6 M^{-1} in isolation, but this value increases by an order of magnitude when the site is in the troponin complex (*5*). NMR measurements have shown that cTnC undergoes a structural change upon binding Ca^{2+}, the extent of which depends on whether it is in isolation or in complex with other proteins (*6, 7*).

The loop of site II is composed of 12 amino acids, six of which (positions 1, 3, 5, 7, 9, and 12) (*8*) coordinate binding of the Ca^{2+} ion with a pentagonal bipyramidal geometry. Several mutagenesis studies have investigated the importance of the acid side chains (positions 1, 3, 9, and 12) responsible for coordinating Ca^{2+} in cTnC (*9*−*11*) and show that the highly conserved aspartate in positions 1 and 3 and the glutamate in position 12 are essential for coordination of Ca^{2+} binding in isolation and in the troponin complex (*10*−*12*). Glycine at position 6 (noncoordinating) is also essential for maintenance of the structure. In fact, this residue is a glycine in 96% of EF-hand loops (*13*). The importance of the coordinating residues at positions 5 and 7 and noncoordinating residues at positions 8, 10, and 11 has not been determined.

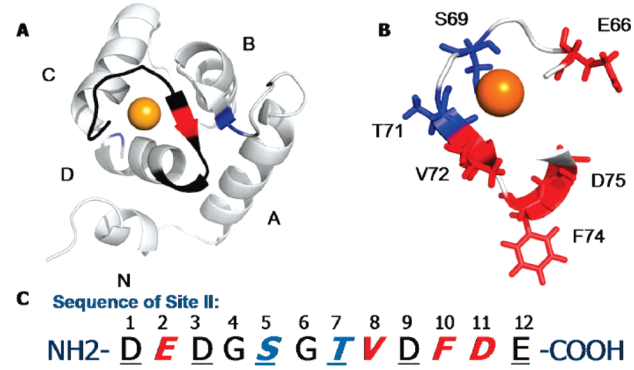

FIGURE 1: Single-cysteine substitutions in site II of cTnC. Panel A shows the N-domain of cTnC with Ca bound at site II. Helices N−D are labeled, and site II is highlighted. Panel B shows the details of site II. Noncoordinating sites of mutation are colored red and coordinating sites blue. Panel C shows the sequence of site II with the mutated residues colored as in panel B. Coordinating residues are underlined.

We have introduced six single-cysteine substitutions within site II of cTnC to investigate whether the specific residues that occupy positions 5 and 7 (S69 and T71, respectively) and noncoordinating residues (E66, V72, F74, and D75) (see Figure 1) are essential determinants of Ca^{2+} binding affinity in isolation and Ca^{2+} sensitivity of force development in single muscle fibers. Mutation of E66 has been investigated previously (*14*). Mutations of aspartic and glutamic acids were avoided since these residues are essential for Ca^{2+}

† This work was supported by the Heart, Lung, and Blood Institute (Grant R37 HL82900).

* To whom correspondence should be addressed. Phone: (608) 262-1939. Fax: (608) 265-5512. E-mail: rlmoss@physiology.wisc.edu.

[1] Abbreviations: cTnC, cardiac/slow skeletal troponin C; skTnC, skeletal troponin C; cTnI, cardiac troponin I; skTnI, fast skeletal troponin I; bc, TnC purified from bovine myocardium; His-wt, recombinant cTnC with an N-terminal His tag.

10.1021/bi800164c CCC: $40.75
Published on Web 04/15/2008

coordination (*15*). Glycine residues were also avoided as these play key structural roles in the formation of the loop (*8*). Although the hydroxyl group on the S69 side chain is known to participate in Ca^{2+} coordination (*8*), it has never been studied using mutagenesis. Cysteine was used for substitution because of its relatively benign side chain and for its potential for chemical modification. The effects of these substitutions on structure and function in solution and when incorporated in single muscle fibers are described.

EXPERIMENTAL PROCEDURES

Mutagenesis, Expression, and Purification. cDNA for wild-type chicken cTnC (provided by H. Cheung) was subcloned into the pQE-30 expression vector (Qiagen), which encodes an N-terminal 6x His tag. Mutagenesis was performed using the QuikChange mutagenesis kit from Stratagene. The two endogenous cysteines (C35 and C84) were mutated to serines, and a single cysteine was substituted at various locations in the regulatory calcium binding loop (site II). cTnC mutants were expressed in *Escherichia coli* and purified from cell lysate using NiNTA resin and buffer solutions from Novagen, and the purity of individual fractions was assessed using SDS−PAGE stained with Coomassie blue. The protein concentration was determined using both absorbance at 276 nm and the method of Bradford (*16*) using a Bio-Rad protein assay kit standardized by comparison with amino acid analysis by acid hydrolysis. Fractions that were >90% pure were pooled and dialyzed against 100 mM KCl, 10 mM MOPS (pH 7.2), and 5 mM EDTA. EDTA [$K_{Ca} = 5.42 \times 10^{10}$; $K_{Mg} = 5.69 \times 10^{8}$ (*17*)] was removed stepwise to reduce the amount of contaminating Ca^{2+} or Mg^{2+} bound to the protein. The final dialysis buffer consisted of 100 mM KCl, 10 mM MOPS (pH 7.2), and 1 mM DTT. Fractions (500 μL) were flash-frozen in liquid N_2 and stored at −80 °C.

Calcium Binding Assay. The Ca^{2+} binding affinity of cTnC mutants was determined using a competition assay as described by Linse (*18*). Protein (1 μM) was mixed with 1 μM Calcium Green 2 (Molecular Probes) in 2 mL of buffer containing 100 mM KCl and 10 mM MOPS (pH 7.2). Aliquots (2 μL) of 500 μM to 10 mM Ca^{2+} were titrated, and changes in fluorescence were measured using a Hitachi F-2000 fluorometer (excitation at 506 nm, emission at 530 nm). Calcium Green 2 was chosen because the $K_{d,Ca^{2+}}$ is similar to that of site II of cTnC, which is important to allow an approximately equal distribution of Ca^{2+} ions between the indicator and protein (*18*). All solutions and proteins were treated with Chelex to remove contaminating calcium. This method reduced the level of contaminating Ca^{2+} to ≤200 nM as measured by fluorescence as described previously (*19*). Ca^{2+} binding affinities were calculated as previously described (*20*) by entering binding equations into Microsoft Excel and using the solver function to determine the dissociation constant of site II of cTnC ($K_{d,II}$). The dissociation constants of tightly coupled, high-affinity sites III and IV ($K_{d,III/IV}$) could not be determined using Calcium Green 2 and were assumed to be 0.2 μM on the basis of measurements taken in previous studies (*5, 20*).

Experimental Solutions. Experimental solutions were prepared using the computer program developed by Fabiato (*21*) and stability constants listed by Godt and Lindley (*22*). Relaxing solution contained 100 mM KCl, 20 mM imidazole, 4 mM MgATP, 2 mM EGTA, and 1 mM free Mg^{2+} (pH 7.0) at 22 °C. Activating solutions contained 100 mM BES (pH 7.2), 7 mM EGTA, 14.5 mM creatine phosphate, and 5 mM DTT. pCa 9.0 contained 21.77 mM potassium propionate, 4.52 mM ATP, 0.042 mM $CaCl_2$, and 5.63 mM $MgCl_2$, while pCa 4.5 contained 9.773 mM potassium propionate, 4.57 mM ATP, 7.06 mM $CaCl_2$, and 5.29 mM $MgCl_2$. Prior to activation in calcium solution, fibers were incubated in a preactivating solution containing 100 mM BES (pH 7.2), 0.07 mM EGTA, 4.5 mM creatine phosphate, 5 mM DTT, 37.73 mM potassium propionate, 4.54 mM ATP, 0 mM calcium chloride, and 5.23 mM $MgCl_2$. Solutions were prepared at 22 °C and adjusted to an ionic strength of 150 mM using potassium propionate. pCa 4.5 and 9.0 were mixed to produce solutions with a range of free Ca^{2+} concentrations.

Skinned Soleus Preparations. Soleus muscle was removed from Sprague-Dawley rats and dissected to bundles of 10 fibers. Fiber bundles were tied to glass capillary tubes and skinned in 1% Triton X-100 (ThermoFisher Scientific) at 4 °C for 4−5 h. Fiber bundles were then transferred to and stored in relaxing solution containing 50% glycerol at −20 °C for up to 2 weeks. Animal usage was conducted in accordance with institutional guidelines using protocols approved by the Animal Care and Use Committees of the University of Wisconsin.

Experimental Protocol for Skinned Fiber Experiments. Single skinned soleus fibers from rats were tied between a force transducer (model 400A, Aurora Scientific) and length controller (model 308B, Aurora Scientific) on an apparatus similar to one previously described (*23*) and stretched to a sarcomere length of 2.55 μm. Steady-state force signals of each fiber were digitized at 1 kHz using a 12-bit A/D converter (model AT-MIO-16F-5, National Instruments Corp.) and displayed and stored on a personal computer using customized software (LabView Full Development System for Windows, version 5.01, National Instruments Corp.). Length changes were driven by computer-generated voltage commands, which were output to the torque motor via a 12-bit D/A converter. All experiments were performed at 22 °C. Sarcomere length and fiber dimensions were monitored throughout the experiment using a video camera (model WV-BL600, Panasonic) mounted on an inverted light microscope (Olympus). Following each experiment, the portion of the fiber between the motor and force transducer was cut and stored in Laemmli sample buffer at −80 °C until it was analyzed by SDS−PAGE (15%) and silver stained (Plus One Silver staining kit, GE Healthcare) (see Figure 2). The N-terminal His tag allowed differentiation of mutant proteins from endogenous cTnC following incorporation into single muscle fibers since the His tag causes the mutants to run higher on the gel (see Figure 2). The amount of cTnC extracted was determined using densitometry. Each mutant isoform of cTnC was tested in at least three fibers.

Extraction of Endogenous TnC and Reconstitution with Recombinant cTnC. After control measurements of steady-state force in solutions with various free Ca^{2+} concentrations, fibers were transferred to a rigor solution [10 mM KCl, 5 mM imidazole (pH 6.8), and 5 mM EDTA] for 2 min, followed by an extracting solution containing 10 mM imidazole (pH 6.8), 5 mM EDTA, and 0.2 mg/mL trifluoperazine in the dark for 60 min. Force was reduced to 30% of

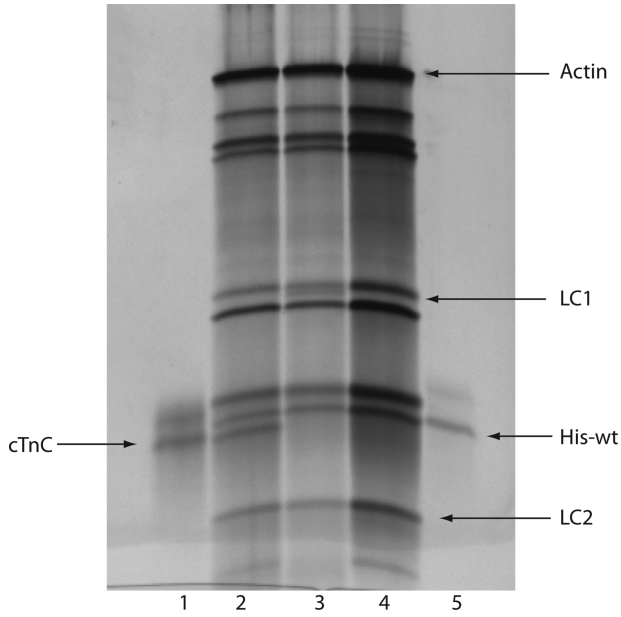

FIGURE 2: TnC content of single soleus fibers. Lane 1 contained purified cTnC. Lane 2 contained a single soleus fiber. Lane 3 contained a soleus fiber following extraction of endogenous TnC. Lane 4 contained a soleus fiber following reconstitution with D75C. Lane 5 contained purified His-wt. His-wt comigrates with possibly a Z-line protein (e.g., T-cap, ~19 kDa) (*54*). The band above the purified TnC bands (lanes 1 and 4) is the Mg^{2+}-bound form of the protein (*55*).

pre-extracted values, and increasing the time of extraction did not result in any further decrease in maximum Ca^{2+}-activated force. The fiber was subsequently washed five times in fresh relaxing solution to remove any residual TFP. Various mutant isoforms of cTnC were reconstituted into TnC-extracted fibers by bathing the fibers in a 1.0 mg/mL protein solution for 20 min, at which point there was no further increase in the maximum Ca^{2+}-activated force. Force was restored to 80% of pre-extracted values. To prevent nonspecific binding, fibers were incubated cyclically in a protein solution for 1 min followed by the relaxing solution for 1 min. Steady-state force was measured again with various free Ca^{2+} concentrations to characterize pCa−force relationships.

Molecular Modeling. cTnC mutations were modeled after available crystal or NMR structures using Deep View (*24*), and energy minimization was performed with SYBYL [specific Protein Data Bank (PDB) entries listed in the text]. Intramolecular interactions were studied using Deep View, and solvent accessibilities were calculated using MolMol (*25*). Solvent accessibilities are calculated by dividing the solvent accessible surface area of a residue in its native state by that of the residue within the protein. Figures were created with PyMol (*26*).

RESULTS

Effects of Single-Cysteine Substitutions on cTnC in Solution. Competition assays with Calcium Green 2 were performed to determine the Ca^{2+} binding affinity of cTnC mutants in isolation in solution. The competition assay allows the Ca^{2+} binding constant to be determined in a manner that is independent of conformational changes. Ca^{2+} was titrated in 2 μL increments (using Ca^{2+} stock solutions of 0.5 μM, 1 μM, 10 μM, and 100 mM), which resulted in a progressive increase in fluorescence. The solution was mixed by aspiration with a pipet and stirred during the titration. The peak fluorescence intensity measured following each Ca^{2+} addition was normalized to the minimum and maximum signals, and these data were plotted versus $-\log_{10}[Ca^{2+}]_{total}$ as shown in Figure 3. The K_d of Calcium Green 2 was calculated to be 1.16 ± 0.11 μM. A mixture of 1 μM cTnC and 1 μM Calcium Green 2 in 100 mM KCl and 10 mM MOPS (pH 7.2) was titrated with Ca^{2+} to determine the K_d of site II of His-tagged, recombinant cTnC (His-wt) (2.10 ± 0.18 μM). His-wt exhibited no significant difference in Ca^{2+} binding affinity as compared to cTnC purified from bovine myocardium (2.24 ± 0.24 μM). Cysteine substitutions E66C, T71C, V72C, F74C, and D75C showed no significant difference in Ca^{2+} binding affinity as compared to His-wt or bovine cTnC (see Table 1).

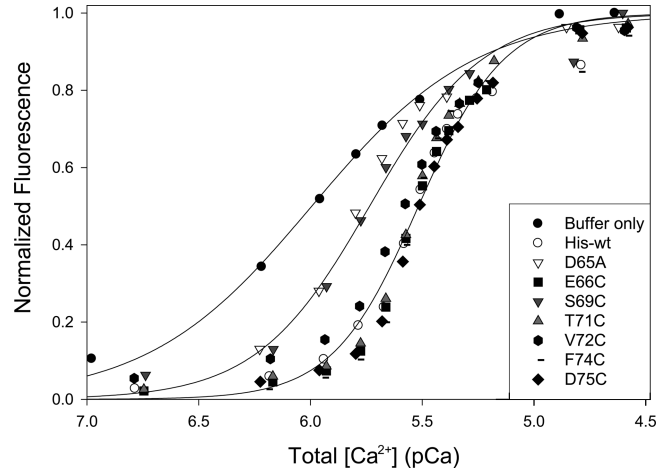

FIGURE 3: Calcium binding to cTnC in solution. Calcium binding affinity was measured for all cTnC mutants. All mutants exhibited similar binding affinities (2−3 μM), except S69C, which did not bind calcium at site II. Binding constants are listed in Table 1. A titration curve for D65A is included as a negative control.

When the coordinating serine at position 69 was substituted (S69C), Ca^{2+} binding at site II was eliminated; however, the mutant in which the coordinating threonine at position 71 was replaced with serine retained Ca^{2+} binding. CBM-II, which contains the D65A mutation (*10, 12, 27*), has been studied extensively, and is known not to bind Ca^{2+} at site II, was used as a control for this assay. The titration curve for D65A is similar to that of S69C (Figure 3). The titration curves indicate that these proteins still bind Ca^{2+} normally at sites III and IV.

Effects of Single-Cysteine Substitutions in Soleus Fibers. Single, skinned soleus fibers from rat were used to assess the function of the mutant cTnCs in situ because soleus fibers contain the cardiac/slow skeletal isoform of TnC. Also, the soleus fiber is very robust in that it can be subjected to long experimental procedures without exhibiting rundown. Endogenous TnC was chemically extracted, and the fiber was reconstituted with the appropriate cTnC isoform. To ensure proteins were being specifically incorporated into the soleus fiber, each fiber was incubated with bovine cTnC following reconstitution with mutant cTnC. If the protein was not properly incorporated, bovine cTnC would have restored Ca^{2+} sensitivity; however, no change was observed in Ca^{2+} sensitivity, maximum Ca^{2+}-activated force, or Hill coefficient.

Table 1: Summary of Mutant Properties[a]

	bovine cTnC	His-wt	E66C	T71C	V72C	F74C	D75C
$K_{d,Ca}$	2.24 ± 0.24	2.20 ± 0.30	1.51 ± 0.22	1.82 ± 0.20	2.05 ± 0.19	1.73 ± 0.33	1.90 ± 0.40
pCa_{50}	6.34 ± 0.03	5.96 ± 0.03	5.92 ± 0.02	5.76 ± 0.01[b]	6.04 ± 0.01[c]	6.24 ± 0.03[b]	6.02 ± 0.02
n_H	1.96 ± 0.03	1.04 ± 0.03	1.32 ± 0.13[c]	1.04 ± 0.04	1.05 ± 0.12	1.17 ± 0.01[c]	1.14 ± 0.04
P_{post}/P_0	89 ± 7	78 ± 4	79 ± 4	76 ± 4	78 ± 2	85 ± 2	79 ± 4

[a] The Ca^{2+} dissociation constants for site II of cTnC mutants ($K_{d,Ca}$) were determined using a competition assay described above (see Figure 3). All values are expressed in micromolar. Ca^{2+} sensitivities of force (pCa_{50}) and Hill coefficients (n_H) were determined following incorporation of cTnC into rat skinned soleus fibers (see Figure 4). pCa_{50} values are expressed as $-\log[Ca^{2+}]$. P_{post}/P_0 refers to the percent of maximum Ca^{2+}-activated force recovered following reconstitution with cTnC mutants. "Bovine cTnC" refers to TnC purified from bovine myocardium. Data are means ± the standard error. [b] For $p < 0.01$. [c] For $0.01 \leq p \leq 0.05$.

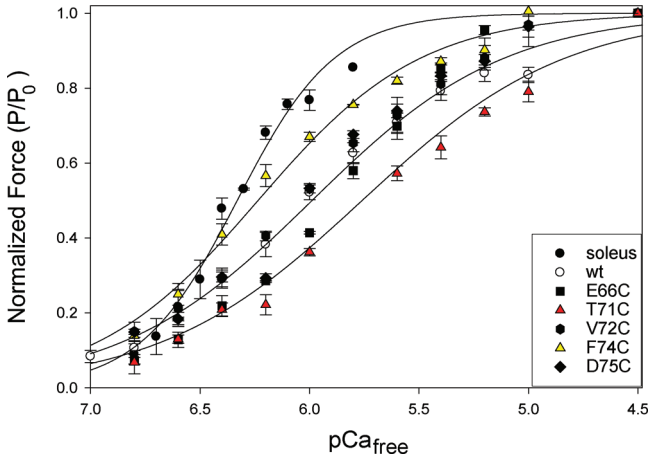

FIGURE 4: Effect of single-cysteine mutants on Ca^{2+} sensitivity. Force vs pCa was measured for each cysteine mutant after incorporation of each mutant cTnC into single soleus fibers. S69C was unable to activate force generation. T71C (red triangles) shows significantly reduced Ca^{2+} sensitivity, while F74C (yellow triangles) shows significantly increased Ca^{2+} sensitivity. Fiber characteristics are given in Table 1. Only one line is drawn to represent E66C, V72C, and D75C for clarity.

The pCa_{50} for His-wt was 5.96 ± 0.03, a right shift in Ca^{2+} sensitivity compared to the control (6.34 ± 0.03), and the slope of the force−pCa curve was reduced to 1.04 ± 0.03 (Figure 4 and Table 1), which is most likely caused by the His tag. However, since all the mutant proteins have the His tag, this shift is expected to be constant. Fibers reconstituted with S69C or D65A were unable to generate force. Ca^{2+} sensitivities of force for E66C (5.92 ± 0.02) and D75C (6.02 ± 0.02) were similar to His-wt. Although T71C (5.76 ± 0.01) bound Ca^{2+} normally in solution, the Ca^{2+} sensitivity of force significantly decreased following reconstitution into soleus fibers compared to His-wt. F74C (6.24 ± 0.03) also bound Ca^{2+} normally in solution but caused a significant increase in Ca^{2+} sensitivity compared to His-wt. V72C (6.04 ± 0.01) exhibited a slight but significant increase in Ca^{2+} sensitivity compared to His-wt. Each soleus fiber generated 80% maximum Ca^{2+}-activated force following reconstitution with mutant cTnC. The slopes of the force−pCa curves for T71C, V72C, and D75C were similar to that of His-wt (Table 1); however, an increase in slope was observed for both E66C (1.32 ± 0.13) and F74C (1.17 ± 0.01).

Structural Effects of Single-Cysteine Substitutions. Each mutation was modeled using Deep View (*24*) in NMR structures of cTnC in isolation with [PDB entry 1AP4 (*28*)] and without [PDB entry 1SPY (*28*)] Ca^{2+} and in the crystal structure of cTnC in the troponin complex [PDB entry 1J1D (*29*)]. Solvent accessibilities were calculated using MolMol (*25*) in each structure and for each mutation (data not shown).

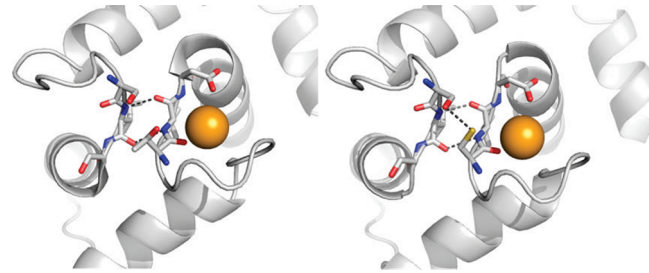

FIGURE 5: Structural effect of the T71C mutation. The N-domain of cTnC is shown bound with Ca^{2+} (orange). The residues of the short, antiparallel β-sheet (C35S-I36-S37 and T71-V72-D73) are represented as "sticks" with the T71C side chain colored yellow. The gray dashes represent the endogenous hydrogen bonds between I36 and V72, and the black dashes represent the possible additional hydrogen bond formed between C35S and T71C (left). The structure was created using PDB entry 1J1D.

There did not appear to be a correlation between changes in function and changes in solvent accessibility. Noncovalent bonding was examined in the Ca^{2+}-saturated models in isolation and in complex using the "show contacts" function in Protein Explorer, and these findings were confirmed in Deep View. There was no apparent change in noncovalent bonding for E66C, V72C, or D75C. As expected, D65A and S69C lost their ability to coordinate Ca^{2+} due to loss of coordinating oxygens. T71C maintains its ability to coordinate Ca^{2+} through the backbone carbonyl both in isolation and in complex, which explains why mutation of this coordinating residue did not affect Ca^{2+} binding in isolation and why this mutant confers Ca^{2+} sensitivity of activation to soleus fibers. Modeling of T71C in the troponin complex revealed the formation of a possible additional H-bond between the cysteine sulfhydryl and the hydroxyl group of C35S of the short antiparallel β-sheet between the T71-V72-D73 sequence and the C35S-I36-S37 sequence (see Figure 5). V72 is a highly conserved residue in EF-hand loops. This position is always a hydrophobic residue and forms two H-bonds with I36 through the backbone carbonyl and amides creating the β-sheet. Substituting cysteine at position 72 does not disrupt this backbone H-bonding. F74 is located in a cluster of phenylalanine residues (residues 20, 24, 27, 74, and 77) in the hydrophobic core (Figure 6). When cTnC is incorporated in the troponin complex, changes in spatial orientation (*30*) bring the F74 side chain closer to F20. The distance between these residues in the structure from PDB entry 1AP4 is 5 Å, while the distance measured between these residues in PDB entry 1J1D is 3.9 Å. The distance measured using PDB entry 1J1D containing the F74C mutation is more than 6 Å. In addition to increasing the distance between these residues, substitution of a polar cysteine residue might interfere with hydrophobic interactions within

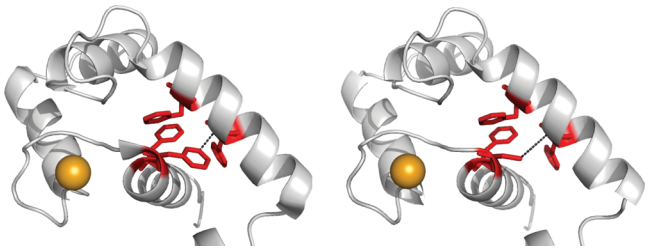

FIGURE 6: Structural effect of the F74C mutation. The N-domain of cTnC is shown bound with Ca^{2+} (orange). F20, F24, F74, and F77 are colored red. The hydrophobic interactions between F20 and F74 (right) are lost with F74C (left). The dashed line represents the change in distance between the F74/F74C side chain and the F20 backbone. The structure was created using PDB entry 1J1D.

the phenylalanine cluster. The amide proton of F74 forms an H-bond with the backbone carbonyl of G34 (*31*), and this interaction is maintained in F74C (see Figure 6).

DISCUSSION

Six single-cysteine substitutions were introduced into site II of cTnC to determine the importance of specific site II residues in Ca^{2+} binding and function. cTnC molecules with mutations at various positions in site II bound Ca^{2+} normally in solution and thus were expected to activate force development normally. Cardiac thin filaments are more sensitive to the activating effects of crossbridges at submaximal Ca^{2+} concentrations than fast skeletal thin filaments, which can be inferred in the less steep force−pCa curve with cardiac muscle fibers (*1, 32, 33*). This effect is, in part, due to differences in structure between fast skeletal (sk) and cTnC (*28, 34, 35*). Ca^{2+} binding to skTnC in isolation induces a large structural change or opening of the N-domain, resulting in lengthening of the molecule (*36*). Ca^{2+} binding to cTnC in isolation results in an only slight structural change, yielding a more compact molecule (*6*). When in complex, this slight opening allows the regulatory region of cTnI (cTnI-R) to bind to the hydrophobic patch on cTnC (*28*). Binding of the inhibitory region of cTnI (cTnI-I) to Ca^{2+}-bound cTnC causes a large structural change similar to that caused by Ca^{2+} binding to skTnC (*37*). This movement drags the rest of the cTnI molecule with it, causing cTnI-I to release actin and free crossbridge binding sites on the thin filament, a mechanism termed "drag and release" (*35, 38*). Although the structures of cTnC and skTnC are similar in the presence of TnI, the mechanisms for the conformational changes are kinetically and thermodynamically different primarily due to the different sequences for site I (*31, 37, 39*). Given that both Ca^{2+} and cTnI are required for full opening of cTnC, the function of cTnC in isolation cannot be directly related to the function of cTnC incorporated into muscle fibers, as the results of this study and other physiological studies demonstrate (*40*−*42*).

For example, Dotson and Putkey (*15*) used mutagenesis to inactivate each binding loop in cTnC. With sites III and IV (N107A and N143A, CBM-III/IV) mutated or with sites II, III, and IV mutated, these proteins bound 1 and 0 mol of Ca^{2+}, respectively, as expected in isolation. However, equilibrium dialysis revealed that Ca^{2+} binding to sites III and IV was restored when the mutants were associated with the Tn complex. Furthermore, CBM-III/IV also showed a recovery of Ca^{2+} binding activity when incorporated into myofibrils, although Ca^{2+} sensitivity was significantly reduced. This phenomenon has also been observed with calmodulin (as described in ref *15*). Haiech et al. (*43*) mutated glutamic acid at position 12 in either loop II or loop IV and serine at position 9 in loop III in calmodulin and assessed Ca^{2+} binding in solution and in the absence and presence of calmodulin binding peptide, RS20. When both sites III and IV were mutated, calmodulin bound 2 mol of Ca^{2+}, indicating that sites III and IV had become inactivated. However, when Ca^{2+} binding was assessed in the presence of the calmodulin binding peptide, RS20, the site III/IV mutant bound 4 mol of Ca^{2+}, indicating that Ca^{2+} binding function had been restored. The study presented here shows the opposite effect: Ca^{2+} binding is normal when cTnC mutants are in isolation but perturbed when they are in complex.

The right shift in Ca^{2+} sensitivity and the decrease in the Hill coefficient in soleus fibers reconstituted with His-wt are most likely due to the N-terminal His tag. If the His tag caused a dramatic structural perturbation, we would expect to see a reduced level of Ca^{2+} binding in isolation as well. Since the N-terminus of cTnC is exposed, this result was unexpected. Analysis of the crystal structure of skTnC in complex with residues 1−47 of skTnI shows that the N-terminal region of skTnI (residues 1−13) has polar and van der Waals interactions with the N-lobe of skTnC (*44*). It is possible that the His tag interferes with this association of TnI, causing the right shift. Although there is a decrease in Ca^{2+} sensitivity in recombinant proteins as compared to bovine cTnC, the effects seen in the mutants are valid since all the proteins have a His tag and would all experience an equal reduction in Ca^{2+} sensitivity. Previously published evidence shows that changes in cTnC function can occur without any structural perturbations. For example, Ca^{2+} binding is abolished in the D65A mutant simply due to loss of the coordinating oxygen and disruption of the hydrogen bonding network in site II without disruption of the β-sheet. NMR showed that this mutant did not change the conformation or stability of the molecule (*30*).

This study shows that S69C abolishes Ca^{2+} binding at site II even though the hydroxyl side chain of Ser is a weaker coordinating group than a carboxylate side chain. While the majority of EF-hand proteins have an Asp or Asn in this position, 20% of EF-hand proteins contain Ser, including parvalbumins (*8, 13*). Ca^{2+} binding loops containing Ser generally H-bond with the coordinating water molecule at position 9 (*45*). The reason calcium binding is abolished with this substitution is most likely a combination of effects from losing the coordinating oxygen and disrupting the H-bonding network since S69 is part of the planar pentagonal coordination unit.

The result that coordinating residue T71C not only bound Ca^{2+} in isolation but also was able to activate force development was unexpected. Although threonine is the most common residue to occupy this position in EF-hand loops, this position is occupied by other residues in 75% of EF-hand proteins, which is consistent with the result that substitution of this residue did not disrupt Ca^{2+} binding (*13*). Results from modeling the mutation in Deep View show that the coordination of Ca^{2+} through the backbone carbonyl of T71C is not disrupted. Spyracopoulos et al. (*31*) showed that unlike skTnC, sites I and II of cTnC are similar in flexibility.

When Ca^{2+} binds, site II becomes more rigid as the residues adopt the appropriate conformation to ligate the Ca^{2+} ion. Site I also becomes more rigid upon binding of Ca^{2+} to site II, indicating that these sites are thermodynamically coupled (*31*). This energy is communicated between sites in part by the small, antiparallel β-sheet comprised of C35, I36, and S37 (mutant proteins contain C35S) in site I and T71, V72, and D73 in site II through H-bonds between V72 and I36. It appears that the T71C side chain forms an additional H-bond with C35S, which is part of the β-sheet. The structural integrity of the Ca^{2+} binding loops is maintained by an extensive H-bonding network (*46*). While this extra H-bond may not disturb Ca^{2+} binding in solution, it could make the association between the two loops more rigid, which possibly limits the extent of structural rearrangements upon binding of TnI.

When Ca^{2+} binds to cTnC in the presence of TnI, there is a helical rearrangement in which helices B and C move as a unit away from helices N, A, and D, which also move as a unit. The loss of the hydrophobic interaction of F74 (D helix) with F20 (A helix) may weaken the interactions in the hydrophobic core, allowing the N-lobe of cTnC to open more freely. In this case, the presence of Ca^{2+} and TnI would confer greater Ca^{2+} sensitivity as observed in soleus fibers. V72C exhibited a small but statistically significant increase in Ca^{2+} sensitivity compared to His-wt. The V72 side chain contributes to the hydrophobic interactions in the hydrophobic core. Like F74C, V72C may disrupt hydrophobic interactions leading to the increase in Ca^{2+} sensitivity. This concept has been demonstrated previously (*47*) when several residues in the hydrophobic pocket were mutated to polar glutamine residues. These substitutions increased Ca^{2+} binding affinity presumably because substitution of a polar residue into a hydrophobic environment makes conformational changes in the N-domain of cTnC more favorable (*47*). Interestingly, the F27W mutant commonly used to measure Ca^{2+} binding properties related to conformational changes in cTnC shows increased Ca^{2+} sensitivity in skinned trabeculae (*41*). It is possible that the bulky tryptophan side chain interferes with the spatial orientation of residues in the N-terminal hydrophobic pocket, causing an effect similar to the effect of substitution of hydrophobic residues with glutamine or cysteine as in this study. It is interesting that since the sequence of site II of cTnC is in a highly conserved region of cTnC, mutating noncoordinating residues E66 and D75 had no effect on Ca^{2+} binding affinity or Ca^{2+} sensitivity (*48*). E66C exhibited an increase in the slope of the force−pCa curve; however, a structural mechanism for this increase is unclear. Dotson and Putkey (*15*) mutated E66 to alanine in rabbit skeletal TnC, and this mutant appeared to function like the wild type, although Hill coefficients were not reported in this study.

Activation of force development depends on both Ca^{2+} and crossbridges. Ca^{2+} is required to initially switch on the thin filament and activate crossbridge cycling. Strong binding of crossbridges creates positive feedback such that strongly bound crossbridges promote binding of additional crossbridges and also increase the level of binding of Ca^{2+} to the thin filament (*49, 50*). The prevailing three-state model for thin filament activation (*51, 52*) includes a blocked state when no Ca^{2+} is present and tropomyosin sterically blocks myosin binding sites on actin, a closed state when Ca^{2+} is present and crossbridges can weakly bind to the thin filament, and an open state in which crossbridges strongly bind to actin. In general, Ca^{2+} binding to TnC causes structural changes that lead to the movement of tropomyosin and exposure of crossbridge binding sites on actin. Similarly, as crossbridges begin to bind, they pin tropomyosin in the open state (*53*), which presumably causes conformational changes in troponin. This mechanism allows communication between Ca^{2+} and crossbridges through tropomyosin (*53*). Since cTnC depends on binding of both Ca^{2+} and TnI to open, it is reasonable to assume that the cardiac thin filament is more responsive to strong binding crossbridges because movement of tropomyosin causes TnI to dissociate from actin and bind to cTnC, forcing it into its open conformation and increasing the apparent binding affinity of cTnC for Ca^{2+}. Recent biochemical (*35*) studies demonstrate that the presence of myosin S1 is required for full opening of cTnC. Based on this reasoning, T71C reduced Ca^{2+} sensitivity in soleus fibers because a possible additional H-bond made the N-domain more rigid, creating a less energetically favorable environment for opening of cTnC and thereby weakening the ability of strongly bound crossbridges to influence cTnC structure. F74C and V72C increased Ca^{2+} sensitivity because the disruption of hydrophobic interactions made the N-domain less rigid, creating a more favorable environment for opening of cTnC and thus making it easier for strongly bound crossbridges to influence cTnC structure. F74C also showed a small increase in the slope of the force−pCa curve. If F74C can undergo structural rearrangement more freely than His-wt, it follows that this mutation may make the system more cooperative.

The effects of substitution of residues in positions 5, 7, 8, 10, and 11 in site II of cTnC were investigated for the first time. Mutation of residues at positions 7 and 10 displayed normal Ca^{2+} binding properties; however, Ca^{2+} sensitivities in soleus fibers were decreased and increased, respectively, due to changes in intramolecular interactions. This study shows that relatively small changes in tertiary structure can disrupt communication between thick and thin filaments.

ACKNOWLEDGMENT

We thank Dr. Herbert Cheung for the cTnC cDNA, Dr. Jeff Walker for helpful suggestions and discussion, and Dr. Brian Sykes for review of the manuscript.

REFERENCES

1. Gordon, A. M., Homsher, E., and Regnier, M. (2000) Regulation of contraction in striated muscle. *Physiol. Rev. 80*, 853–924.
2. Kobayashi, T., and Solaro, R. J. (2005) Calcium, thin filaments, and the integrative biology of cardiac contractility. *Annu. Rev. Physiol. 67*, 39–67.
3. Leavis, P. C., and Kraft, E. L. (1978) Calcium Binding to Cardiac Troponin C. *Arch. Biochem. Biophys. 186*, 411–415.
4. van Eerd, J. P., and Takahashi, K. (1975) The amino acid sequence of bovine cardiac troponin-C. Comparison with rabbit skeletal troponin-C. *Biochem. Biophys. Res. Commun. 64*, 122–127.
5. Potter, J. D., and Gergely, J. (1975) The calcium and magnesium binding sites on troponin and their role in the regulation of myofibrillar adenosine triphosphatase. *J. Biol. Chem. 250*, 4628–4633.

6. Sia, S. K., Li, M. X., Spyracopoulos, L., Gagne, S. M., Liu, W., Putkey, J. A., and Sykes, B. D. (1997) Structure of cardiac muscle troponin C unexpectedly reveals a closed regulatory domain. *J. Biol. Chem. 272*, 18216–18221.
7. Dong, W. J., Xing, J., Villain, M., Hellinger, M., Robinson, J. M., Chandra, M., Solaro, R. J., Umeda, P. K., and Cheung, H. C. (1999) Conformation of the regulatory domain of cardiac muscle troponin C in its complex with cardiac troponin I. *J. Biol. Chem. 274*, 31382–31390.
8. Boguta, G., and Bierzynski, A. (1988) Conformational properties of Ca^{2+}-binding segments of proteins from the troponin C superfamily. *Biophys. Chem. 31*, 133–137.
9. Wang, S., George, S. E., Davis, J. P., and Johnson, J. D. (1998) Structural determinants of Ca^{2+} exchange and affinity in the C terminal of cardiac troponin C. *Biochemistry 37*, 14539–14544.
10. Putkey, J. A., Sweeney, H. L., and Campbell, S. T. (1989) Site-directed Mutation of the Trigger Calcium-binding Sites in Cardiac Troponin C. *J. Biol. Chem. 264*, 12370–12378.
11. Babu, A., Su, H., and Gulati, J. (1993) The mechanism of Ca^{2+}-coordination in the EF-hand of TnC, by cassette mutagenesis. *Adv. Exp. Med. Biol. 332*, 125–131.
12. Putkey, J. A., Liu, W., and Sweeney, H. L. (1991) Function of the N-terminal Calcium-binding Sites in Cardiac/Slow Troponin C Assessed in Fast Skeletal Muscle Fibers. *J. Biol. Chem. 266*, 14881–14884.
13. Gifford, J. L., Walsh, M. P., and Vogel, H. J. (2007) Structures and metal-ion-binding properties of the Ca^{2+}-binding helix-loop-helix EF-hand motifs. *Biochem. J. 405*, 199–221.
14. Babu, A., Su, H., Ryu, Y., and Gulati, J. (1992) Determination of residue specificity in the EF-hand of troponin C for Ca^{2+} coordination, by genetic engineering. *J. Biol. Chem. 267*, 15469–15474.
15. Dotson, D. G., and Putkey, J. A. (1993) Differential recovery of Ca^{2+} binding activity in mutated EF-hands of cardiac troponin C. *J. Biol. Chem. 268*, 24067–24073.
16. Bradford, M. M. (1976) A rapid and sensitive method for the quantitation of microgram quantities of protein utilizing the principle of protein-dye binding. *Anal. Biochem. 72*, 248–254.
17. Martell, A. E., and Smith, R. M. (1974) *Critical Stability Constants*, Vol. 1, Plenum Press, New York.
18. Linse, S. (2002) Calcium binding to proteins studied via competition with chromophoric chelators. *Methods Mol. Biol. 173*, 15–24.
19. Reece, K. L., and Moss, R. L. (2007) Removal of contaminating calcium from buffer solutions used in calcium binding assays. *Anal. Biochem. 365*, 274–276.
20. Hazard, A. L., Kohout, S. C., Stricker, N. L., Putkey, J. A., and Falke, J. J. (1998) The kinetic cycle of cardiac troponin C: Calcium binding and dissociation at site II trigger slow conformational rearrangements. *Protein Sci. 7*, 2451–2459.
21. Fabiato, A. (1988) Computer programs for calculating total from specified free or free from specified total ionic concentrations in aqueous solutions containing multiple metals and ligands. *Methods Enzymol. 157*, 378–417.
22. Godt, R. E., and Lindley, B. D. (1982) Influence of temperature upon contractile activation and isometric force production in mechanically skinned muscle fibers of the frog. *J. Gen. Physiol. 80*, 279–297.
23. Moss, R. L. (1979) Sarcomere length-tension relations of frog skinned muscle fibres during calcium activation at short lengths. *J. Physiol. 292*, 177–192.
24. Guex, N., and Peitsch, M. C. (1997) SWISS-MODEL and the Swiss-PdbViewer: An environment for comparative protein modeling. *Electrophoresis 18*, 2714–2723.
25. Koradi, R., Billeter, M., and Wuthrich, K. (1996) MOLMOL: A program for display and analysis of macromolecular structures. *J. Mol. Graphics 14*, 29–32., 51−55.
26. DeLano, W. L. (2002) The PyMOL Molecular Graphics System, DeLano Scientific, Palo Alto, CA.
27. Butters, C. A., Tobacman, J. B., and Tobacman, L. S. (1997) Cooperative effect of calcium binding to adjacent troponin molecules on the thin filament-myosin subfragment 1 MgATPase rate. *J. Biol. Chem. 272*, 13196–13202.
28. Spyracopoulos, L., Li, M. X., Sia, S. K., Gagne, S. M., Chandra, M., Solaro, R. J., and Sykes, B. D. (1997) Calcium-induced structural transition in the regulatory domain of human cardiac troponin C. *Biochemistry 36*, 12138–12146.
29. Takeda, S., Yamashita, A., Maeda, K., and Maeda, Y. (2003) Structure of the core domain of human cardiac troponin in the Ca^{2+}-saturated form. *Nature 424*, 35–41.
30. Brito, R. M., Krudy, G. A., Negele, J. C., Putkey, J. A., and Rosevear, P. R. (1993) Calcium plays distinctive structural roles in the N- and C-terminal domains of cardiac troponin C. *J. Biol. Chem. 268*, 20966–20973.
31. Spyracopoulos, L., Gagne, S. M., Li, M. X., and Sykes, B. D. (1998) Dynamics and thermodynamics of the regulatory domain of human cardiac troponin C in the apo- and calcium-saturated states. *Biochemistry 37*, 18032–18044.
32. Swartz, D. R., and Moss, R. L. (1992) Influence of a strong-binding myosin analogue on calcium-sensitive mechanical properties of skinned skeletal muscle fibers. *J. Biol. Chem. 267*, 20497–20506.
33. Fitzsimons, D. P., Patel, J. R., and Moss, R. L. (2001) Cross-bridge interaction kinetics in rat myocardium are accelerated by strong binding of myosin to the thin filament. *J. Physiol. 530*, 263–272.
34. Swartz, D. R., Moss, R. L., and Greaser, M. L. (1996) Calcium alone does not fully activate the thin filament for S1 binding to rigor myofibrils. *Biophys. J. 71*, 1891–1904.
35. Robinson, J. M., Dong, W. J., Xing, J., and Cheung, H. C. (2004) Switching of troponin I: Ca^{2+} and myosin-induced activation of heart muscle. *J. Mol. Biol. 340*, 295–305.
36. Herzberg, O., Moult, J., and James, M. N. (1986) A model for the Ca^{2+}-induced conformational transition of troponin C. A trigger for muscle contraction. *J. Biol. Chem. 261*, 2638–2644.
37. Li, M. X., Spyracopoulos, L., and Sykes, B. D. (1999) Binding of cardiac troponin-I147−163 induces a structural opening in human cardiac troponin-C. *Biochemistry 38*, 8289–8298.
38. Li, M. X., Wang, X., and Sykes, B. D. (2004) Structural based insights into the role of troponin in cardiac muscle pathophysiology. *J. Muscle Res. Cell Motil. 25*, 559–579.
39. Spyracopoulos, L., Lavigne, P., Crump, M. P., Gagne, S. M., Kay, C. M., and Sykes, B. D. (2001) Temperature dependence of dynamics and thermodynamics of the regulatory domain of human cardiac troponin C. *Biochemistry 40*, 12541–12551.
40. Davis, J. P., Rall, J. A., Alionte, C., and Tikunova, S. B. (2004) Mutations of Hydrophobic Residues in the N-terminal Domain of Troponin C Affect Calcium Binding and Exchange with the Troponin C-Troponin I96−148 Complex and Muscle Force Production. *J. Biol. Chem. 279*, 17348–17360.
41. Norman, C., Rall, J. A., Tikunova, S. B., and Davis, J. P. (2007) Modulation of the Rate of Cardiac Muscle Contraction by Troponin C Constructs with Various Calcium Binding Affinities. *Am. J. Physiol. 293*, H2580−H2587.
42. Kreutziger, K. L., Gillis, T. E., Davis, J. P., Tikunova, S. B., and Regnier, M. (2007) Influence of enhanced troponin C Ca^{2+}-binding affinity on cooperative thin filament activation in rabbit skeletal muscle. *J. Physiol. 583*, 337–350.
43. Haiech, J., Kilhoffer, M. C., Lukas, T. J., Craig, T. A., Roberts, D. M., and Watterson, D. M. (1991) Restoration of the calcium binding activity of mutant calmodulins toward normal by the presence of a calmodulin binding structure. *J. Biol. Chem. 266*, 3427–3431.
44. Vassylyev, D. G., Takeda, S., Wakatsuki, S., Maeda, K., and Maeda, Y. (1998) Crystal structure of troponin C in complex with troponin I fragment at 2.3-Å resolution. *Proc. Natl. Acad. Sci. U.S.A. 95*, 4847–4852.
45. Strynadka, N. C., and James, M. N. (1989) Crystal structures of the helix-loop-helix calcium-binding proteins. *Annu. Rev. Biochem. 58*, 951–998.
46. Krudy, G. A., Brito, R. M., Putkey, J. A., and Rosevear, P. R. (1992) Conformational changes in the metal-binding sites of cardiac troponin C induced by calcium binding. *Biochemistry 31*, 1595–1602.
47. Tikunova, S. B., and Davis, J. P. (2004) Designing calcium sensitizing mutations in the regulatory domain of cardiac troponin C. *J. Biol. Chem. 279*, 35341–35352.
48. Gillis, T. E., Marshall, C. R., and Tibbits, G. F. (2007) Functional and Evolutionary Relationships of Troponin C. *Physiol. Genomics 32*, 16–27.
49. Brenner, B. (1988) Effect of Ca^{2+} on cross-bridge turnover kinetics in skinned single rabbit psoas fibers: Implications for regulation of muscle contraction. *Proc. Natl. Acad. Sci. U.S.A. 85*, 3265–3269.
50. Campbell, K. (1997) Rate constant of muscle force redevelopment reflects cooperative activation as well as cross-bridge kinetics. *Biophys. J. 72*, 254–262.

51. McKillop, D. F., and Geeves, M. A. (1993) Regulation of the interaction between actin and myosin subfragment 1: Evidence for three states of the thin filament. *Biophys. J. 65*, 693–701.
52. Maytum, R., Lehrer, S. S., and Geeves, M. A. (1999) Cooperativity and switching within the three-state model of muscle regulation. *Biochemistry 38*, 1102–1110.
53. Tobacman, L. S., and Butters, C. A. (2000) A new model of cooperative myosin-thin filament binding. *J. Biol. Chem. 275*, 27587–27593.
54. Pyle, W. G., and Solaro, R. J. (2004) At the crossroads of myocardial signaling: The role of Z-discs in intracellular signaling and cardiac function. *Circ. Res. 94*, 296–305.
55. Reinach, F. C., and Karlsson, R. (1988) Cloning, Expression, and Site-directed Mutagenesis of Chicken Skeletal Muscle Troponin C. *J. Biol. Chem. 263*, 2371–2376.

BI800164C